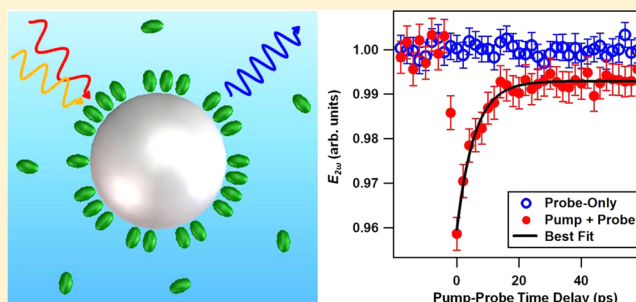


Molecular Excited-State Relaxation Dynamics at the Colloidal Microparticle Interface Monitored with Pump–Probe Second Harmonic Generation

Louis H. Haber[†] and Kenneth B. Eisenthal*

Department of Chemistry, Columbia University, New York, New York 10027, United States

ABSTRACT: Time-resolved second harmonic generation is used to monitor the excited-state relaxation dynamics of molecules adsorbed to the surface of colloidal microparticles suspended in solution. The cationic organic dye, malachite green (MG), is adsorbed to the negatively charged surface of polystyrene sulfate microparticles in water. MG is photoexcited to the S_1 excited state by a 615 nm pump pulse. The time-dependent change of the S_0 ground-state depletion is probed by second harmonic generation of an 800 nm pulse as a function of pump–probe delay to obtain a lifetime of 5.7 ± 0.4 ps. This excited-state lifetime is approximately three times longer than the corresponding lifetime at the air/water interface, showing the significant effect of the negatively charged surface on local friction, which is important in the energy relaxation of photoexcited MG.



1. INTRODUCTION

Understanding the chemical and physical properties of molecules at the surface of microparticles or nanoparticles in solution is of fundamental scientific interest and is important for the development and optimization of applications in a broad range of fields such as catalysis, photovoltaics, and biology.^{1–4} Second harmonic generation (SHG), where two incident photons of frequencies ω combine to generate a photon at frequency 2ω ,^{5,6} is a powerful technique for studying molecules at the interface of colloidal particles and the liquid in which they are suspended.⁴ Coherent SHG is forbidden in bulk media that have inversion symmetry or are isotropic. However, SHG can be generated at the surface of centrosymmetric particles of size that is roughly the length scale of the incident light. Thus SHG is a surface-sensitive spectroscopy that can probe the surface of small, nano- to micro-sized centrosymmetric particles.^{7,8}

Previous SHG studies on colloids have investigated adsorption isotherms of molecules to the surface of colloidal particles made of polystyrene,^{9–14} clay,¹⁵ TiO_2 ,¹⁶ carbon black,¹⁷ gold,¹⁸ and silver.¹⁹ Kinetic SHG measurements have investigated processes such as molecular transport across a liposome membrane^{20,21} as well as enzyme binding, cutting, and rehybridization of DNA attached to microparticles²² on the time scales of seconds to hours. SHG spectroscopy, obtained by scanning the fundamental laser frequency, has measured the electric quadrupole plasmon energy of colloidal silver nanoparticles²³ and the spectrum of the charge-transfer complex of catechol on colloidal TiO_2 particles.¹⁶ The interference between the dipole and octupole SHG response from spherical gold nanoparticles has been determined under varying input polarizations for comparison to theoretical predictions.²⁴ SHG

measurements have also been used to obtain the electrostatic potential²⁵ and surface acidity pK_a value²⁶ of charged colloidal particle surfaces. In addition, by measuring the angular scattering dependence of SHG from colloidal particles,^{27–30} information on the molecular orientation distribution at the particle surface has been recently determined.³⁰

Time-resolved second harmonic generation (TR-SHG) and time-resolved sum frequency generation (TR-SFG) are established techniques for studying molecular dynamics at planar interfaces such as the air/water interface.^{31–33} TR-SHG has been used to investigate molecular rotational dynamics,³⁴ relaxation dynamics of electronic molecular excited-states,^{35–40} electron and energy transfer between molecules,⁴¹ and solvation dynamics^{42,43} at the air/water and liquid/liquid interfaces. Recent work has also used TR-SHG to determine the orientational distribution of molecules⁴⁴ and the formation dynamics of hydrated electrons⁴⁵ at the air/water interface. Ultrafast dynamics of electron and hole carriers at solid state interfaces in organic light-emitting diodes,⁴⁶ fullerene/polyimide double-layers,⁴⁷ and quantum dot thin films on titanium dioxide⁴⁸ have been studied using time-resolved electric-field induced second harmonic generation measurements. On much longer time scales of minutes to hours, TR-SHG has been used to study DNA hybridization at fused quartz/aqueous interfaces.⁴⁹

Special Issue: B: Paul F. Barbara Memorial Issue

Received: May 2, 2012

Revised: August 13, 2012

Published: August 28, 2012



In this paper, the excited-state relaxation dynamics of molecules adsorbed to a colloidal microparticle surface have been studied for the first time using time-resolved second harmonic generation. The cationic organic dye malachite green, adsorbed to the negatively charged surface of 1 μm polystyrene sulfate microparticles in water, is investigated by pump–probe SHG to obtain the molecular excited-state lifetime at the colloidal interface. The method of TR-SHG uniquely probes the molecules at the microparticle surface and not in the bulk due to the nonlinear symmetry restrictions, gaining an advantage over other methods such as transient absorption and streak-field fluorescence, which can be largely dominated by molecules in the bulk solution. For this reason, TR-SHG promises to be an important technique for future studies of molecular dynamics at colloidal microparticle and nanoparticles surfaces.

2. EXPERIMENTAL SECTION

The experimental setup, shown schematically in Figure 1, utilizes a pump–probe configuration for time-resolved second

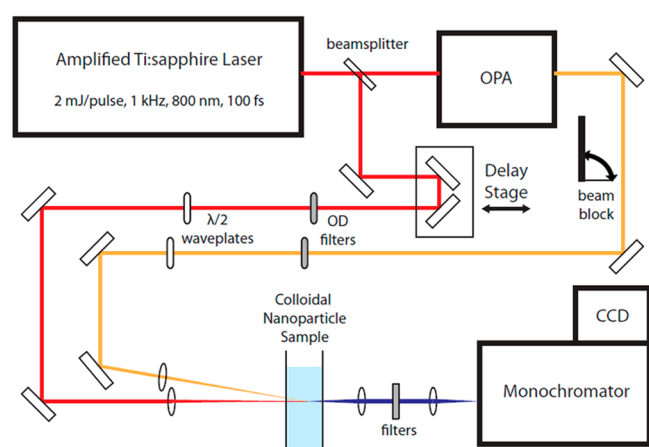


Figure 1. Pump–probe SHG experimental setup for colloidal microparticle samples.

harmonic generation measurements of a colloidal microparticle or nanoparticle sample. An amplified titanium:sapphire laser system produces 2 mJ, 100 fs pulses centered at 800 nm with a 1 kHz repetition rate. A 70:30 beam splitter separates the pump and probe beams, respectively. The pump beam is sent through an optical parametric amplifier (OPA) for the generation of the 615 nm pump pulses, while the 800 nm probe beam is sent to a retroreflector on a delay stage that controls the relative pump–probe temporal delay. Positive pump–probe times correspond to the pump pulse arriving prior to the probe pulse at the sample. Both pump and probe pulses are attenuated with optical density filters to 3 and 2 μJ , respectively, before being focused using 16 and 12 cm lenses, respectively, to a spatial overlap at a relative angle of 5 degrees at the center of a 1 cm fused quartz cuvette containing the colloidal microparticle sample. The second harmonic generation of the probe pulse is collected in the forward direction and dielectric filters are used to remove the pump and fundamental probe wavelengths. The SHG spectra are detected using a monochromator in front of a high-sensitivity charge-coupled device spectroscopy camera connected to a computer. A beam block opens and shuts on the pump pulse in synchronization with an automated file saving program to record the probe-only and pump + probe

SHG spectra for each pump–probe time delay. In the data presented here, 19 scans of 39 time steps ranging from -18 to $+58$ ps are recorded using 5 s acquisitions of pump-only and pump + probe spectra for each time step for statistical analysis.

The colloidal microparticles used in the experiments are 1.06 ± 0.02 μm diameter monodisperse polystyrene sulfate microspheres purchased from Polysciences, Inc. The microparticles are diluted to 3×10^7 particles/mL in nanopure water and the pH is adjusted to 4.3 with HCl. The cationic molecular dye, malachite green, is added to a concentration of 2 μM . The sulfate groups at the particle surface provide an attractive negatively charged interface for the adsorption of the cationic MG molecules in solution. These conditions correspond to a freely adsorbed MG molecular monolayer of a density of approximately 5×10^{13} cm^{-2} at the microparticle surface.¹⁰

3. RESULTS AND DISCUSSION

The pump–probe SHG experimental results provide for the surface-specific relaxation dynamics of molecules at the colloidal microparticle interface. The pump and probe pulse wavelengths are carefully chosen to study the malachite green molecule. The pump pulse wavelength of 615 nm photoexcites MG from the S_0 ground state to the S_1 excited state, causing a time-dependent depletion and recovery of the ground-state population. The SHG photon energy at 400 nm corresponds to the two-photon transition from the S_0 ground state to the S_2 excited state. By varying the pump–probe time delay, the time-dependent ground-state depletion and recovery is directly measured to obtain the relaxation dynamics of the S_1 photoexcited MG molecule at the microparticle interface.

Representative SHG spectra are shown in Figure 2 at two different pump–probe time delays. Both the probe-only and

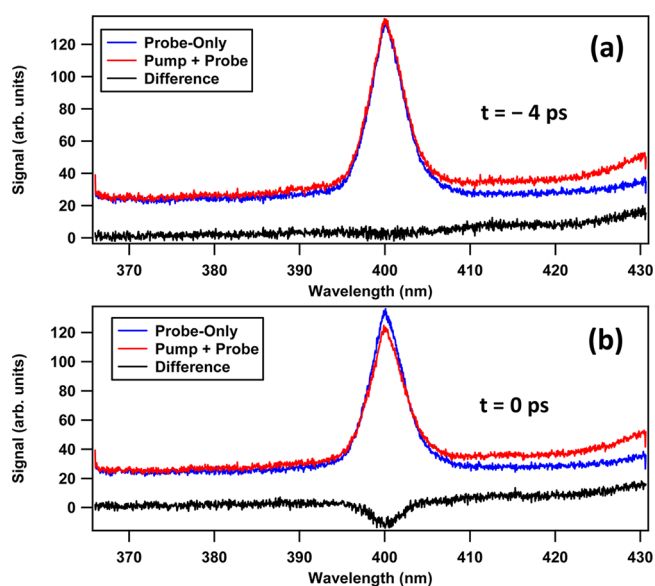


Figure 2. Probe-only, pump + probe, and difference spectra at (a) -4 and (b) 0 ps.

the pump + probe SHG spectra are shown for the time delays of (a) -4 and (b) 0 ps. All SHG spectra are centered at 400 nm, corresponding to twice the probe pulse frequency. At -4 ps, the probe pulse arrives prior to the pump pulse, so there is no ground-state depletion and therefore no change in the SHG signal. However at 0 ps, the pump + probe SHG signal is clearly

lower than the probe-only signal due to the ground-state depletion by the S_0 to S_1 pump-pulse photoexcitation. The time-independent deviation between the probe-only and pump + probe spectra at longer wavelengths in Figure 2 is due to the incomplete filtering of the pump wavelength, and is easily discriminated from the spectra so that this additional signal does not affect the time-resolved SHG experimental results.

The second harmonic generation signal is proportional to the square of the second harmonic (SH) electric field, $E_{2\omega}$. The SH electric field is proportional to the second-order polarization, $P_{2\omega}^{(2)}$, given by

$$E_{2\omega} \approx P_{2\omega}^{(2)} = \chi^{(2)} E_{\omega} E_{\omega}$$

where E_{ω} is the incident electromagnetic field and $\chi^{(2)}$ is the second-order susceptibility, which contains information on the molecular adsorbate. In a pump–probe time-resolved SHG measurement, the total time-dependent second-order susceptibility can be expressed by

$$\chi^{(2)}(t) = \chi_g^{(2)}(t) + \chi_e^{(2)}(t)$$

where $\chi_g^{(2)}(t)$ and $\chi_e^{(2)}(t)$ are the time-dependent second-order susceptibilities of the ground and excited states, respectively. Figure 3 shows $E_{2\omega}$ as a function of the pump–probe time

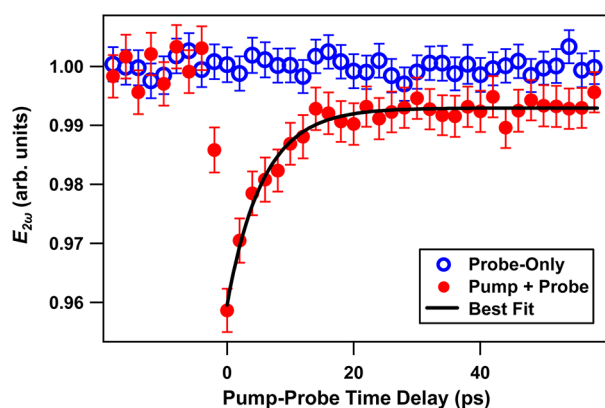


Figure 3. SH electric field, $E_{2\omega}$, as a function of pump–probe time delay from the probe-only (open blue circles) and the pump + probe (closed red circles) spectra. $E_{2\omega}$ of the pump + probe is proportional to the MG ground-state population, showing the depletion and recovery dynamics.

delay for both the probe-only and the pump + probe signal. The probe-only $E_{2\omega}$ is constant, as expected, showing the laser and sample stability. The pump + probe $E_{2\omega}$ shows no depletion at negative time delays, as expected, and it then shows a maximum ground-state depletion at $t = 0$, with a subsequent ground-state recovery at later times. The experimental results of the pump + probe $E_{2\omega}$ measurements are fit to a single exponential given by $Ae^{-t/\tau} + B$, where τ is the measured lifetime. The best fit gives a lifetime of $\tau = 5.7 \pm 0.4$ ps. The amplitudes of A and B are -0.033 ± 0.001 and 0.993 ± 0.001 , respectively, where the signals are normalized to the probe-only $E_{2\omega}$. The origin of the offset B is not known at this time; possibilities include long-lived relaxations that are not currently resolved temporally due to limitations in the optical setup.

The relaxation dynamics of the MG S_1 excited state in bulk solutions and at planar interfaces have been studied extensively in previous investigations.^{35–37,50} The S_1 excited state under-

goes an ultrafast transition to the ground state characterized by the torsional motions of the three aromatic rings around the central carbon, with lifetimes that depend on the local friction experienced by the MG molecule.^{35–38,50} In two separate transient absorption studies of MG in bulk water, the relaxation dynamics were fit to three exponential decay times ranging from 0.3 to 2.4 ps.^{36,37,50} The two longer decay times are found to increase with increasing macroscopic bulk viscosity in bulk water and glycerol mixtures, consistent with a model of a torsional isomerization of the aromatic rings in the excited state first twisting away from the ground-state conformation and then twisting back in the ground-state recovery.^{37,50}

Surface-selective pump–probe second harmonic generation measurements allow for the determination of the MG excited-state molecular dynamics at different air/liquid, liquid/liquid, and solid/liquid interfaces. The S_1 excited-state lifetimes are found to be longer at the air/water interface than in bulk water, which is attributed to the increased local friction of the MG molecule at the air/water interface.^{35,36,50} Additionally, the corresponding excited-state lifetimes are found to increase at the alkane/water interface, showing a general trend of longer lifetimes with increasing alkane chain lengths.^{35,38} The MG S_1 excited-state lifetime is even longer at the silica/water interface and is attributed to restricted torsional motions due to the electrostatic attraction of the cationic dye to the negatively charged sites on the silica surface leading to hindered molecular dynamics.³⁵ Finally, much longer MG excited-state lifetimes on the order of hundreds of picoseconds are observed at significantly increased salt concentrations and are attributed to dye aggregation.^{36,38} The S_1 excited-state lifetimes of MG at the air/water, octane/water, pentadecane/water, and silica/water planar interfaces have been previously determined to be 2.0 ± 0.3 , 3.0 ± 0.4 , 3.6 ± 0.3 , and 5.5 ± 1.0 ps, respectively.³⁵ These results at the air/water and alkane/water interfaces are similar to other TR-SHG measurements^{36,38} when converting the biexponential decays to single exponential fits for direct comparisons. The MG excited-state lifetime at the colloidal polystyrene sulfate microparticle surface in water, measured here to be 5.7 ± 0.4 ps, is two to three times longer than the corresponding values at the air/water and alkane/water interfaces, and is within the experimental error of the corresponding lifetime at the silica/water interface.

The findings show that the electrostatic attraction of the cationic dye to negatively charged surfaces for both polystyrene sulfate/water and silica/water is an important factor that contributes to the observed significant increase in the molecular excited-state lifetimes. The detailed interplay between intramolecular forces involving the torsional isomerization of the aromatic rings around the central carbon and the intermolecular interactions of the MG molecule with solvent molecules at the interface, including solvation dynamics as well as orientational dynamics of MG at the interface, is important for a full description of the local friction experienced by the molecule. In addition to the restricted torsional and rotational motions of the MG molecule due to electrostatic forces at the surface, the positive and negative charge distributions can alter the hydrogen-bonding networks in the water, leading to higher local viscosities and contributing to the observed increase in excited-state lifetimes. The influence of the surface-specific electrostatic attraction on the hindered torsional dynamics in the molecular excited-state relaxation requires future experimental and theoretical studies.

4. CONCLUSIONS

The excited-state relaxation dynamics of molecules adsorbed to the surface of colloidal microparticles have been measured for the first time using time-resolved second harmonic generation. The S_1 excited-state lifetime of malachite green at the surface of polystyrene sulfate microparticles suspended in water has been determined to be 5.7 ± 0.4 ps. This lifetime is longer than the corresponding results at the air/water and alkane/water interfaces by a factor of two to three, and is within experimental error of the MG lifetime at the water/silica interface, which is negatively charged. The results indicate that it is the difference in the local friction at the interface that is responsible for the observed lifetimes. The torsional motions of the phenyl groups attached to the central carbon effect the change in structure in making the transition from the excited state potential energy surface to the ground electronic state where the phenyl groups are in a "propeller orientation" with respect to each other. The attractive interaction between the positively charged MG and the negatively charged polystyrene sulfate could impose a restriction on the orientation of MG, and thus restrict the orientation of the phenyl groups that would inhibit the torsional motions necessary for the relaxations. These results demonstrate that the surface-sensitive time-resolved technique of pump–probe second harmonic generation is a powerful method for future investigations of molecular dynamics at colloidal microparticle and nanoparticle interfaces.

AUTHOR INFORMATION

Corresponding Author

*E-mail: kbe1@columbia.edu. Phone: (212) 854-3175.

Present Address

[†]Department of Chemistry, Louisiana State University, Baton Rouge, Louisiana 70803, United States.

Notes

The authors declare no competing financial interest.

ACKNOWLEDGMENTS

The authors would like to thank Yi Rao, Benjamin Doughty, and Sheldon Kwok for many helpful discussions. The authors gratefully acknowledge support from the National Science Foundation (CHE-1057483), the Chemical Sciences, Geosciences and Bioscience Division, Office of Basic Energy Sciences, Office of Science of the U.S. Department of Energy, and DTRA (W911NF-07-1-0116).

REFERENCES

- (1) Kamat, P. V. *J. Phys. Chem. C* **2007**, *111*, 2834–2860.
- (2) Sperling, R. A.; Gil, P. R.; Zhang, F.; Zanella, M.; Parak, W. J. *Chem. Soc. Rev.* **2008**, *37*, 1896–1908.
- (3) Anderson, N. A.; Lian, T. *Annu. Rev. Phys. Chem.* **2005**, *56*, 491–519.
- (4) Eienthal, K. B. *Chem. Rev.* **2006**, *106*, 1462–1477.
- (5) Shen, Y. R. *The Principles of Nonlinear Optics*; Wiley: New York, 1985.
- (6) Shen, Y. R. *Annu. Rev. Phys. Chem.* **1989**, *40*, 327–350.
- (7) Dadap, J. I.; Shan, J.; Eienthal, K. B.; Heinz, T. F. *Phys. Rev. Lett.* **1999**, *83*, 4045–4048.
- (8) Dadap, J. I.; Shan, J.; Heinz, T. F. *J. Opt. Soc. Am. B* **2004**, *21*, 1328–1347.
- (9) Wang, H.; Yan, E. C. Y.; Liu, Y.; Eienthal, K. B. *Chem. Phys. Lett.* **1996**, *259*, 15–20.
- (10) Wang, H.; Yan, E. C. Y.; Liu, Y.; Eienthal, K. B. *J. Phys. Chem. B* **1998**, *102*, 4446–4450.
- (11) Wang, H.; Troxler, T.; Yeh, A.-G.; Dai, H.-L. *Langmuir* **2000**, *16*, 2475–2481.
- (12) Eckenrode, H. M.; Dai, H.-L. *Langmuir* **2004**, *20*, 9202–9209.
- (13) Eckenrode, H. M.; Jen, S.-H.; Han, J.; Yeh, A.-G.; Dai, H.-L. *J. Phys. Chem. B* **2005**, *109*, 4646–4653.
- (14) Schürer, B.; Peukert, W. *Particulate Sci. Tech.* **2010**, *28*, 458–471.
- (15) Yan, E. C. Y.; Eienthal, K. B. *J. Phys. Chem. B* **1999**, *103*, 6056–6060.
- (16) Liu, Y.; Dadap, J. I.; Zimdars, D.; Eienthal, K. B. *J. Phys. Chem. B* **1999**, *103*, 2480–2486.
- (17) Wang, H.; Troxler, T.; Yeh, A.-G.; Dai, H.-L. *J. Phys. Chem. C* **2007**, *111*, 8708–8715.
- (18) Haber, L. H.; Kwok, S. J. J.; Semeraro, M.; Eienthal, K. B. *Chem. Phys. Lett.* **2011**, *507*, 11–14.
- (19) Gan, W.; Gonella, G.; Zhang, M.; Dai, H.-L. *J. Chem. Phys.* **2011**, *134*, 041104–1–3.
- (20) Srivastava, A.; Eienthal, K. B. *Chem. Phys. Lett.* **1998**, *292*, 345–351.
- (21) Liu, J.; Subir, M.; Nguyen, K.; Eienthal, K. B. *J. Phys. Chem. B* **2008**, *112*, 15263–15266.
- (22) Doughty, B.; Kazer, S. W.; Eienthal, K. B. *Proc. Natl. Acad. Sci.* **2011**, *108*, 19979–19984.
- (23) Hao, E. C.; Schatz, G. C.; Johnson, R. C.; Hupp, J. T. *J. Chem. Phys.* **2002**, *117*, 5963–5966.
- (24) Butet, J.; Bachelier, G.; Russier-Antoine, I.; Jonin, C.; Benichou, E.; Brevet, P.-F. *Phys. Rev. Lett.* **2010**, *105*, 077401–1–4.
- (25) Yan, E. C. Y.; Liu, Y.; Eienthal, K. B. *J. Phys. Chem. B* **1998**, *102*, 6331–6336.
- (26) Subir, M.; Liu, J.; Eienthal, K. B. *J. Phys. Chem. C* **2008**, *112*, 15809–15812.
- (27) Yang, N.; Angerer, W. E.; Yodh, A. G. *Phys. Rev. Lett.* **2001**, *87*, 103902–1–4.
- (28) Shan, J.; Dadap, J. I.; Stiofkin, I.; Reider, G. A.; Heinz, T. F. *Phys. Rev. A* **2006**, *73*, 023819–1–4.
- (29) Jen, S.-H.; Gonella, G.; Dai, H.-L. *J. Phys. Chem. A* **2009**, *113*, 4758–4762.
- (30) Gonella, G.; Dai, H.-L. *Phys. Rev. B* **2011**, *84*, 121402–1–5.
- (31) Eienthal, K. B. *Chem. Rev.* **1996**, *96*, 1343–1360.
- (32) Rao, Y.; Song, D.; Turro, N. J.; Eienthal, K. B. *J. Phys. Chem. B* **2008**, *112*, 13572–13576.
- (33) Rao, Y.; Turro, N. J.; Eienthal, K. B. *J. Phys. Chem. C* **2010**, *114*, 17703–17708.
- (34) Shang, X.; Nguyen, K.; Rao, Y.; Eienthal, K. B. *J. Phys. Chem. C* **2008**, *112*, 20375–20381.
- (35) Shi, X.; Borguet, E.; Tarnovsky, A. N.; Eienthal, K. B. *Chem. Phys.* **1996**, *205*, 167–178.
- (36) Punzi, A.; Martin-Gassin, G.; Grilj, J.; Vauthey, E. *J. Phys. Chem. C* **2009**, *113*, 11822–11829.
- (37) Fita, P.; Punzi, A.; Vauthey, E. *J. Phys. Chem. C* **2009**, *113*, 20705–20712.
- (38) Fedoseeva, M.; Fita, P.; Punzi, A.; Vauthey, E. *J. Phys. Chem. C* **2010**, *114*, 13774–13781.
- (39) Fita, P.; Fedoseeva, M.; Vauthey, E. *Langmuir* **2011**, *27*, 4645–4652.
- (40) Martin-Gassin, G.; Villamaina, D.; Vauthey, E. *J. Am. Chem. Soc.* **2011**, *133*, 2358–2361.
- (41) McArthur, E. A.; Eienthal, K. B. *J. Am. Chem. Soc.* **2006**, *128*, 1068–1069.
- (42) Benderskii, A. V.; Eienthal, K. B. *J. Phys. Chem. A* **2002**, *106*, 7482–7490.
- (43) Benderskii, A. V.; Henzie, J.; Baus, S.; Shang, X.; Eienthal, K. B. *J. Phys. Chem. B* **2004**, *108*, 14017–14024.
- (44) Rao, Y.; Hong, S.-Y.; Turro, N. J.; Eienthal, K. B. *J. Phys. Chem. C* **2011**, *115*, 11678–11683.
- (45) Sagar, D. M.; Bain, C. D.; Verlet, J. R. R. *J. Am. Chem. Soc.* **2010**, *132*, 6917–6919.
- (46) Taguchi, D.; Inoue, S.; Zhang, L.; Li, J.; Wies, M.; Manaka, T.; Iwamoto, M. *J. Phys. Chem. Lett.* **2010**, *1*, 803–807.

- (47) Zhang, L.; Taguchi, D.; Manaka, T.; Iwamoto, M. *J. Appl. Phys.* **2011**, *110*, 033715–1–8.
- (48) Tisdale, W. A.; Williams, K. J.; Timp, B. A.; Norris, D. J.; Aydil, E. S.; Zhu, X.-Y. *Science* **2010**, *328*, 1543–1547.
- (49) Boman, F. C.; Gibbs-Davis, J. M.; Heckman, L. M.; Stepp, B. R.; Nguyen, S. T.; Geiger, F. M. *J. Am. Chem. Soc.* **2009**, *131*, 844–848.
- (50) Sen, P.; Yamaguchi, S.; Tahara, T. *Faraday Discuss.* **2010**, *145*, 411–428.